Role of Residue 138 in the Interdomain Hinge Region in Transmitting Allosteric Signals for DNA Binding in *Escherichia coli* cAMP Receptor Protein[†]

Shaoning Yu and J. Ching Lee*

Department of Human Biological Chemistry and Genetics, The University of Texas Medical Branch at Galveston, Galveston, Texas 77555-1055

Received December 9, 2003; Revised Manuscript Received February 19, 2004

ABSTRACT: The cAMP receptor protein (CRP) of *Escherichia coli* is a transcription factor. The affinity of CRP for a specific DNA sequence is significantly enhanced as a consequence of the binding of the allosteric effector, cAMP. The hinge region, particularly residues 136 and 138, connecting the cAMP and DNA binding domains of CRP has been proposed to play essential roles in transmitting the allosteric signals. To probe the specific role of residue 138, eight D138 mutants and wild-type CRP were tested for their ability to bind the lac26 and gallac26 promoter sequences in this study. A correlation was established between DNA binding affinity and side chain solvation free energy, namely, an increasing specific DNA affinity with an increasing hydrophilicity of the side chain of residue 138. In addition, a linear correlation was found between DNA binding affinity and the energetics of subunit assembly. The ability of CRP to distinguish between cAMP and cGMP as an allosteric activator of DNA binding is weakened with higher energetics of subunit assembly. This correlation indicates that quaternary constraint leads to a constraint of the DNA binding domain. This observation is consistent with the concept that an optimum quaternary structural constraint is important in CRP exhibiting its allosteric properties. The stability of CRP was monitored by Trp fluorescence and circular dichroism in the presence of guanidine hydrochloride. These spectroscopic data revealed nonidentical denaturation profiles. Since the Trp residues are located exclusively in the β-roll cyclic nucleotide binding domain, the denaturation profiles reveal the stability of the β-roll structure. This study produces another linear correlation between DNA binding affinity in the presence of cAMP and cGMP and the stability of the β-roll; namely, the stability of the β-roll structure leads to a decrease in DNA binding affinity. All these correlations indicate the importance of structural stability and dynamics in the ability of CRP to manifest its intrinsic allosteric properties.

The expression of more than 100 genes that are involved in different cellular functions in *Escherichia coli* is regulated by cAMP[1] receptor protein (CRP) (*1−5*). Since its isolation in the 1970s, CRP has become one of the most studied transcriptional regulators and the focus of many genetic, biochemical, and biophysical studies (*6−15*). CRP is a dimeric protein composed of two chemically identical subunits with 209 amino acid residues each (*16*). Each subunit contains two domains: a larger N-terminal domain which contains the characteristic cAMP binding β-roll structure and a smaller C-terminal domain which binds to DNA through a helix−turn−helix motif. The two functional domains are connected by a hinge region (residues 135−138) (*7, 17, 18*), as shown in Figure 1.

It has been well-documented that CRP, upon cAMP binding, undergoes allosteric conformational changes that enable the protein to recognize specific DNA sequences. Thus, intersubunit and interdomain communications must be affected by cAMP binding. The crystallographic structure of the CRP−cAMP₂ complex shows that cAMP is buried within the large domain, at least 10 Å from either the DNA binding domain or the hinge region. Consequently, cAMP binding is not likely to affect the domain or subunit rearrangement by direct interaction. This signal transmission process is most likely the net result of long-range communications resulting in an overall realignment of the two subunits within a CRP dimer (*5, 8, 12, 19*). What is the pathway through which CRP transmits the allosteric signal from the cAMP-binding pocket to the DNA binding motif? Does it involve the hinge region (*13, 14, 20−23*)?

Recent studies concluded that loop 3 in the β-roll is involved in both interdomain and intersubunit interaction and is important for the transmission of the cAMP binding signal (*24*). The interaction between loop 3 and F136, which is located in the interdomain hinge region, as shown in Figure 1, might play an important role in these processes. On the basis of the structure of holo-CRP, Passer *et al.* (*7*) proposed that loop 3 collapses into the cAMP-binding pocket in apo-CRP. Such a change would result in the loss of many

* To whom correspondence should be addressed. Phone: (409) 772-2281. Fax: (409) 772-4298. E-mail: jclee@utmb.edu.

[1] Abbreviations: cAMP, 3′,5′-cyclic adenosine monophosphate; cGMP, 3′,5′-cyclic guanosine monophosphate; cCMP, 3′,5′-cyclic cytidine monophosphate; cNMP, 3′,5′-cyclic nucleotide monophosphate; WT, wild type; CPM, *N*-{4-[7-(diethylamino)-4-methylcoumarin-3-yl]-phenyl}maleimide; TEK100, 50 mM Tris, 1 mM EDTA, and 100 mM KCl at pH 7.8 and 25 °C; PAGE, polyacrylamide gel electrophoresis; IPTG, isopropyl thiogalactopyranoside; HTP, hydroxyapatite gel; ANS, 8-anilino-1-naphthalenesulfonic acid magnesium salt; PMSF, phenyl-methanesulfonyl fluoride.
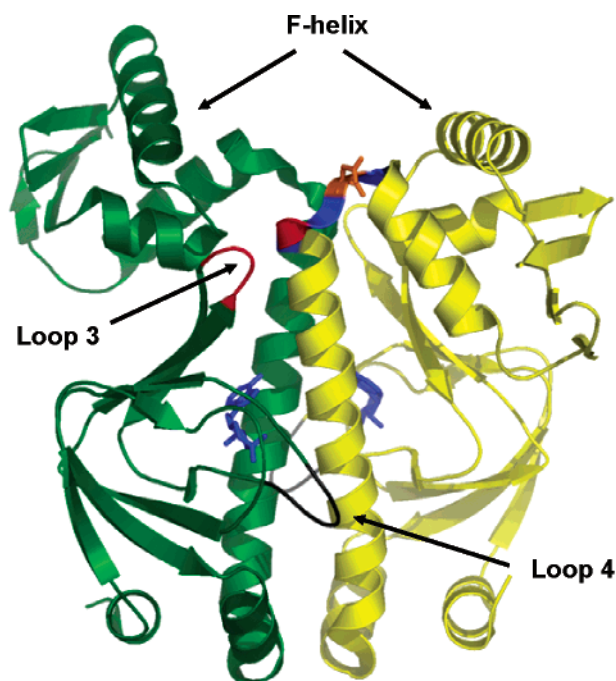
FIGURE 1: Structure of the CRP dimer showing the locations of loops 3 and 4. Subunits 1 and 2 are green and yellow, respectively. The hinge region of adjacent subunit 2 is blue. Residues 136 and 138 in the hinge region of adjacent subunit 2 are red and orange, respectively. cAMP molecules in both subunits are blue.

interactions between one subunit and the C-helix of the adjacent subunit, including the removal of F136 from its contact with loop 3. This interaction could lead to a reorientation of the C-helices and, hence, a reorientation of subunits. The collapse of loop 3 into the empty cAMP-binding pocket would be accompanied by a breaking of the interaction between loop 3 and the small domain. The NMR data showing that the structure around the cAMP-binding pocket of CRP is perturbed by cAMP binding (*8*) are consistent with the proposed structural changes.

Loop 3, C-helices, and the hinge region are involved in the allosteric signal transmission process. In-depth studies have shown that mutations in loop 3, including residues 52, 53, and 62, lead to significant modulation of the thermodynamically linked equilibria which govern the function of CRP (*25*, *26*). Some *in vivo* studies indicated that the hinge region also plays a pivotal role in transmitting allosteric signals to different regions of the protein (*20*, *21*). D138, which is close to F136 and located in the end of the hinge region, is partially exposed to the solvent (Figure 1). What role does residue 138 play in the allosteric signal transmission process? How do residue 138 mutants perturb the interaction between the proposed loop 3−F136 interactions? Does residue 138 affect the CRP conformation by changing the extent of exposure to solvent? Is there any correlation between the side chain properties of residue 138 and protein functions? All these questions remain unanswered. In this *in vitro* study, eight D138 mutants were investigated to probe the effects of hydrophobic, polar, and positively charged side chains on the functional and structural energetics of CRP.

MATERIALS AND METHODS

Materials. cAMP, cCMP, and cGMP were purchased from Sigma (St. Louis, MO). CPM was purchased from Molecular

Probes (Eugene, OR). The absorption coefficients of cyclic nucleotides and fluorescence probes were 14 650 $M^{-1} cm^{-1}$ at 259 nm, 12 950 $M^{-1} cm^{-1}$ at 254 nm, 9100 $M^{-1} cm^{-1}$ at 271 nm, and 33 000 $M^{-1} cm^{-1}$ at 385 nm for cAMP, cGMP, cCMP, and CPM, respectively. Ultrapure guanidine-HCl was a product of ICN Biochemical. Oligonucleotides (lac26, gal26, and gallac26) were purchased from Sigma, and the single-stranded oligo was labeled with CPM at the 5′-end as described previously (*11*, *23*). All experiments were conducted in TEK100 buffer (50 mM Tris, 1 mM EDTA, and 100 mM KCl at pH 7.8 and 25 °C).

Site-Directed Mutagenesis. The Promega Altered Site *in vitro* Mutagenesis System was used to introduce specific point mutations into the crp gene using a previously published procedure (*5*, *23*, *25*). The desired mutants were directly screened by DNA sequencing.

GuHCl Preparation. GuHCl (7.82 M) in TEK100 buffer stock solution was prepared and filtered with a 0.45 μm filter. The concentration of GuHCl was determined by density measurement with an Anton-Paar densimeter. A CRP/GuHCl solution was prepared with stock CRP in a TEK100 solution and GuHCl in a TEK100 solution. The solution was incubated for more than 24 h before being used.

Protein Preparation. Wild-type CRP and all residue 138 mutants were purified from IPTG-induced *E. coli* strain HMS174DE3 with a published procedure (*5*, *25*). The purity of the protein was judged with an SDS−PAGE gel stained with Coomassie blue. The purified protein was stored in a −20 °C freezer with ∼0.2 M KCl and ∼10% glycerol at pH 7.5. The CRP solution was dialyzed against TEK100 buffer overnight to remove the stabilizing agent (glycerol) and other additives with three buffer changes before being used. The concentration of the stock CRP solution was determined spectrophotometrically by using an extinction coefficient of 40 800 $M^{-1} cm^{-1}$ at 278 nm for the CRP dimer (*25*). The ratio of absorbance at 278 nm to that at 260 nm was greater than 1.85, indicating that contaminated DNA was removed. A solution with a high protein concentration was obtained by eluting the adsorbed protein on a HTP column. Mass spectrometry was employed to further check the mass of all mutants (*25*, *26*).

Circular Dichroism Spectroscopy. CD measurements were performed on an AVIV model 60 DS spectropolarimeter. CD spectra of CRP in the native state were measured over the range of 190−340 nm by using 0.01 cm (far-UV, 190−240 nm) and 1.0 cm (near-UV, 240−340 nm) path length cells. Each spectrum was recorded in 0.5 nm wavelength increments. For each sample, three repetitive scans were obtained and averaged. Protein solutions with a concentration of ∼10 μM were used.

DNA Binding. The fluorescence anisotropy experiment was used for quantitative measurement of the CRP−DNA reaction in the presence of cNMP at specified concentrations. DNA sequences are 5′-ATTAA<u>TGTGA</u>GTTAGC<u>TCACT</u>-CATTA-3′ for lac26, 5′-AAAAG<u>TGTGA</u>CATGGAATAAA-TTAGT-3′ for gal26, and 5′-AAAAG<u>TGTGA</u>CATGGAT-<u>CACT</u>TTAGT-3′ for gallac26. The underlined sequences are the primary binding sites for CRP. The reaction mixture contained the CPM-labeled 26 bp fragment of DNA (18−23 nM), 200 μM cNMP, and various amounts of CRP (0−10 μM). Small volumes of concentrated CRP, ranging from 0.2 to 250 μM, were titrated into the reaction mixture in

1−5 μL aliquots. The total volume change that occurred in one titration curve should be as low as possible (<6%). The experiment was conducted in the SLM 8000c spectrofluorometer (*11, 25*). The excitation wavelength was 390 nm, and an oriel band-pass filter (model 59816) was placed in the excitation path to reduce second-order scatter. Oriel hand-pass filters (model 59850) were placed in the emission paths to monitor the total emission from 470 to 570 nm. The anisotropy of the CPM-labeled DNA was measured after each addition of protein. Experimental data were fitted to the following equation by nonlinear least-squares to determine the apparent association constant K_x:

$$A = A_D + (A_{PD} - A_D)$$
$$\left(\frac{K_x D_T + K_x P_T + 1 - \sqrt{K_x D_T + K_x P_T + 1 - 4K_x D_T P_T}}{2K_x D_T} \right) \quad (1)$$

where A is the measured anisotropy, A_D and A_{PD} are values of anisotropy associated with free DNA and the CRP−DNA complex, respectively, D_T and P_T are the total molar concentrations of DNA and the dimeric protein, respectively, and x is A, C, or G (cAMP, cCMP, or cGMP, respectively) (*25*).

Subunit Association. To provide information about the quaternary structure of CRP mutants, the molecular weights of CRP at different GuHCl concentrations were determined by sedimentation equilibrium with the previously published procedures (*23, 27, 28*). Sedimentation equilibrium experiments of each mutant were conducted at 25 000 rpm to determine the apparent association constant at different GuHCl concentrations. The apparent weight-average molecular weights were obtained by fitting the sedimentation equilibrium data with the following equation:

$$C = E + C_{1,r_0} \exp\left[\frac{(1 - \bar{v}\rho)\omega^2}{2RT} M(r^2 - r_0^2) \right] + $$
$$C_{2,r_0}{}^2 K_a \exp\left[\frac{(1 - \bar{v}\rho)\omega^2}{2RT} 2M(r^2 - r_0^2) \right] \quad (2)$$

where C is the observed CRP concentration in absorbance at radial position r, E is the baseline offset, and C_{1,r_0} and C_{2,r_0} are the CRP concentrations of monomeric and dimeric CRP, respectively. At the meniscus r_0, $\bar{v}$ is the partial specific volume, ρ is the solvent density, ω is the angular velocity, M is the apparent weight-average molecular weight, and R and T are the gas constant and temperature in kelvin, respectively. K_a is the apparent association constant. The $\bar{v}$ value of CRP in Tris buffer is 0.745, derived from the amino acid composition of CRP using the method of Cohn and Edsall (*29*).

Protein Unfolding. GuHCl-induced CRP unfolding was carried out with CD and fluorescence spectroscopy. In a typical denaturation experiment, 32 samples at a fixed CRP concentration (∼10 μM) in TEK100 were mixed with varying amounts of a stock GuHCl solution to final GuHCl concentrations ranging from 0 to 6 M. CD spectra of CRP in differential concentrations of GuHCl were measured over the range of 208−250 nm by using the 0.1 cm cell, and two repetitive scans were obtained and averaged. The spectral region close to 250 nm was unchanged and very close to zero. These have been used as the standard to judge the
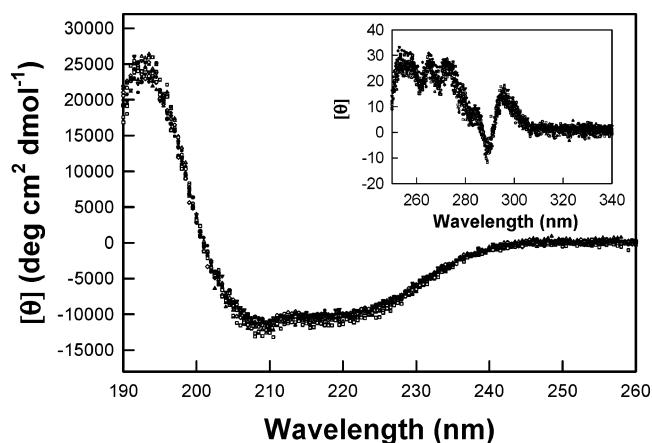

FIGURE 2: CD spectra of WT (●), D138G (▲), D138A (■), D138V (◆), D138L (◇), D138S (△), D138T (□), D138Q (▽), and D138K (+), in TEK100 buffer. Insets are the corresponding signals in the near-UV region. Protein concentrations are ∼10 μM.

quality of these spectra. CD ellipticity at 222 nm was used as a signal to monitor unfolding. The fluorescence intensity was recorded with an SLM 8000 spectrofluorometer at 25 °C. The excitation and emission wavelengths were 285 and 345 nm, respectively.

RESULTS

Structure of CRP Mutants. To examine the structural integrity of all 138 mutants, the overall secondary structure was determined with both near- and far-UV CD spectra. The spectra of the wild type (WT) and residue 138 mutants were presented as typical results, as shown in Figure 2. Both the near- and far-UV CD spectra are essentially identical to each other and to those of wild-type CRP. These results indicate that replacement of Asp with Gly, Ala, Val, Leu, Ser, Thr, Gln, and Lys does not elicit any observable difference in the net content of secondary and tertiary structure of CRP.

DNA Binding. One of the central functions of CRP is to recognize a specific DNA sequence. The affinities of all the residue 138 mutants for lac26 and gallac26 CPM-labeled DNA in the presence of different cNMPs were determined. Figure 3 shows results for the D138G mutant binding to different DNA sequences in the presence of 200 μM cAMP. These results indicate that D138G CRP exhibits the strongest and lowest affinity for the gallac26 and gal26 sequences, respectively. The apparent DNA binding constants of all the residue 138 mutants in the presence of 200 μM cNMP are summarized in Table 1. Because of the low affinity, results of gal26 binding could not be measured with accuracy and therefore are not reported. The values of the corresponding ΔG for all reactions calculated from the binding constant are also shown in Table 1. Significantly, the mutants with a hydrophobic residue at position 138 exhibited lower affinity for both lac26 and gallac26 promoter sequences than wild-type CRP. A positively charged residue exhibited a higher DNA binding affinity. When DNA binding constants for CRP in the presence of cAMP or cGMP were compared, a more than 2000-fold difference was obtained for the polar or positively charged residues, suggesting that these mutants, just like WT CRP, are highly selective for cyclic nucleotide. The order of DNA binding affinity is as follows: D138K > WT ∼ D138Q ∼ D138S ∼ D138T > D138G > D138L ∼ D138A > D138V.
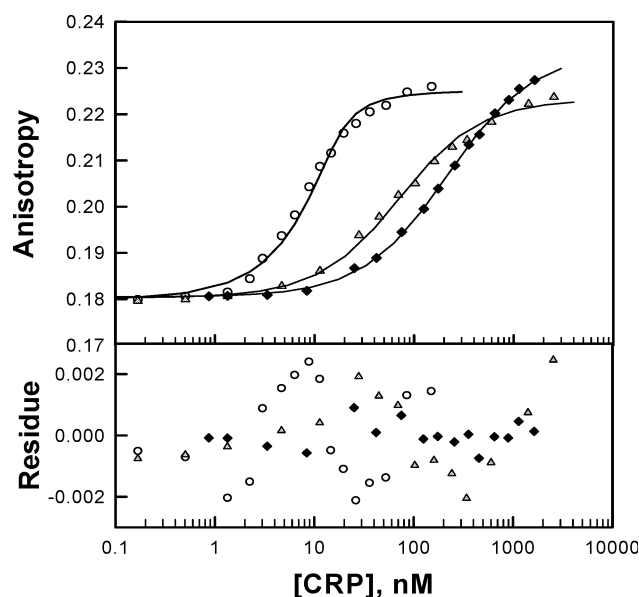
FIGURE 3: Typical binding isotherms for binding of D138G CRP to DNA in TEK100 buffer and 200 μM cAMP at pH 7.8 and 25 °C. The anisotropy of CPM-labeled DNA was normalized to 0.1800. The symbols and corresponding DNA are as follows: (○) gallac26, (△) lac26, and (◆) gal26. The solid line represents the best fit of the data to eq 1.

Subunit Association. The subunit association of CRP is strong, and the presence of denaturant is necessary to weaken the subunit assembly, enabling the association−dissociation reaction to be monitored. However, the subunit dissociation is coupled with protein unfolding in the presence of denaturant, leading to complication in data analysis due to the thermodynamic linkage of these coupled reactions. Thus, the subunit dissociation monitored by the sedimentation method is an apparent parameter. A study of subunit association as a function of denaturant concentration can provide data for extrapolation to infinite dilution of denaturant to yield the energetics of subunit association in buffer. Cheng and Lee (23) have shown that the value of ΔG in buffer determined by this procedure for the residue 141 mutant is identical to that determined directly in the absence of denaturant. Results of residue 138 mutants as well as that of WT for comparison are shown in Figure 4. It is clear that mutations affect the energetics of subunit assembly, since the value of [GuHCl]$_m$, the concentration of denaturant at which CRP exists as a mixture of 50% monomer and dimer, depends on the specific mutant. The data were further analyzed to estimate the apparent dimer association constant at each GuHCl concentration, and the constant K_a was converted to ΔG_a. A plot of ΔG_a versus GuHCl concentration displays a linear relationship. Extrapolation of the data to zero GuHCl concentration yields a value of $\Delta G_a°$ in buffer, as shown in Table 2. These data imply that replacement of Asp with Ala, Val, or Ser significantly enhances the association affinity of subunits, and replacement of Asp with Gly, Leu, Thr, Gln, or Lys does not significantly change it. The mutant with a high subunit association affinity requires a higher GuHCl concentration to induce a 50% mixture of monomer and dimer, as shown in Table 2. Replacement of Asp with Ala or Val transforms a region consisting of residues 134−139 to six consecutive hydrophobic residues (LAFLA/VV). In turn, these hydrophobic residues most likely would be involved

in a strong hydrophobic interaction near the hinge region between two subunits, making it more difficult to dissociate.

Protein Stability. Protein stability studies were conducted to provide information about the folding stability of CRP and possibly domain−domain interaction. Two spectroscopic methods, namely, fluorescence emission intensity at 384 nm and CD absorption at 222 nm, were used to monitor the denaturation of CRP. Methods and procedures for data analysis were the same as those previously published (28). The protein concentration was ~10 μM in a dimeric state. The unfolding curves, as monitored by fluorescence and CD, are shown in Figure 5. The excitation wavelength of fluorescence was 287 nm. The observed data would reflect the microenvironments of the aromatic side chains, which include all tryptophans (at positions 13 and 85) and four of five tyrosines (at positions 23, 41, 63, 99, and 206) located in the cAMP binding domain. Thus, it is highly probable that the denaturation profiles defined by the fluorescence data reflect primarily the unfolding of the cAMP binding domain, whereas the unfolding data from the CD experiment, which provide information about the backbone secondary structure, reflect the events associated with both domains.

The unfolding curve monitored by fluorescence emission intensity is significantly sharper, showing a narrow range of GuHCl concentrations within which the structural transition occurred. Furthermore, it is most interesting to note that the transition curves are essentially identical for all residue 138 mutants. These results imply that the cAMP binding domain unfolds as a cooperative unit and the mutations at residue 138 do not have a significant effect on the stability of the cAMP binding domain.

The unfolding curves monitored by CD exhibit more characteristics that are dependent on the nature of the mutation. In all cases, the transition zone expands to a large range of GuHCl concentrations, indicating a more complex event is being monitored. With the exceptions of the data for D138A and D138V, the CD data indicate the beginning of an unfolding at GuHCl concentrations lower than those detected by fluorescence. Since the unfolding was monitored at 222 nm, the unfolding of α-helices probably is predominantly reflected in these unfolding profiles. The earlier unfolding revealed by CD might indicate the unfolding of the small amount of α-helices in the cAMP binding domain. The unfolding profiles at higher GuHCl concentrations are more complicated and exhibited significant deviation from the profiles determined by fluorescence. The transitions are more gradual with respect to GuHCl concentration. The data for D138A and D138V mutants show the greatest deviations, indicating a stabilization of regions of CRP by these mutations. The detailed information about free energy change and GuHCl concentrations at which 50% of CRP was unfolded are summarized in Table 3. Both CD and fluorescence data showed that D138V, D138A, and D138S are more stable against denaturant than other mutants.

DISCUSSION

Identification of pathways of signal transmission in proteins, particularly in systems exhibiting an allosteric regulatory mechanism, provides important information for an insightful understanding of the mechanism of protein function. Loop 3 in the β-roll cAMP binding domain has

Table 1: Affinity of CRP−lac26 and −gallac26 DNA Complex Formation in the Presence of 200 μM cNMP

oligo and CRP mutants		cAMP		cCMP		cGMP	
		K_{app} ($\times 10^{-6}$ M^{-1})	$-\Delta G$ (kcal/mol)	K_{app} ($\times 10^{-6}$ M^{-1})	$-\Delta G$ (kcal/mol)	K_{app} ($\times 10^{-6}$ M^{-1})	$-\Delta G$ (kcal/mol)
Lac	WT	72.9 ± 5.7	10.7	0.086−0.168[a]	6.7[c]	0.003−0.041	4.7
	D138G	16.4 ± 1.6	9.8	0.004−0.010	4.9	0.001−0.007	4.1
	D138A	0.09 ± 0.01	6.7	0.004−0.008	5.0	0.013 ± 0.018	5.6
	D138V	0.005−0.025	5.1	N[b]	/	0.005−0.020	5.0
	D138L	0.033 ± 0.036	6.2	N[b]	/	0.003−0.023	4.7
	D138S	13.4 ± 1.4	9.7	0.007−0.047	5.3	0.005−0.050	5.0
	D138T	65.2 ± 2.2	10.7	0.18 ± 0.05	7.2	0.002−0.051	4.5
	D138Q	15.1 ± 1.0	9.8	0.40 ± 0.03	7.6	0.004−0.031	5.0
	D138K	1074 ± 41	12.3	0.45 ± 0.04	7.7	0.132 ± 0.035	7.0
Gallac	WT	>2000	12.9	N[b]	/	0.080 ± 0.011	6.7
	D138G	767 ± 268	12.1	0.041 ± 0.009	6.3	0.016 ± 0.005	5.7
	D138A	1.73 ± 0.10	8.5	0.409 ± 0.069	7.7	0.013 ± 0.018	5.6
	D138V	0.080 ± 0.015	6.7	N[b]	/	0.004−0.013	4.9
	D138L	6.24 ± 0.25	9.3	N[b]	/	0.046 ± 0.015	6.4
	D138S	645 ± 178	12.0	0.033−0.022	6.2	0.011 ± 0.040	5.5
	D138T	>2000	13.5	0.018 ± 0.016	5.8	0.002−0.035	4.6
	D138Q	1151 ± 746	12.4	0.26 ± 0.03	7.4	N[b]	/
	D138K	>2000	13.2	20.3 ± 1.5	9.9	2.85 ± 0.29	8.8

[a] A range for the binding constant was reported due to the lack of accuracy in measuring the level of low-affinity binding. The lowest value was used to calculate ΔG. [b] Cannot be measured due to protein aggregation. [c] Minimum value.
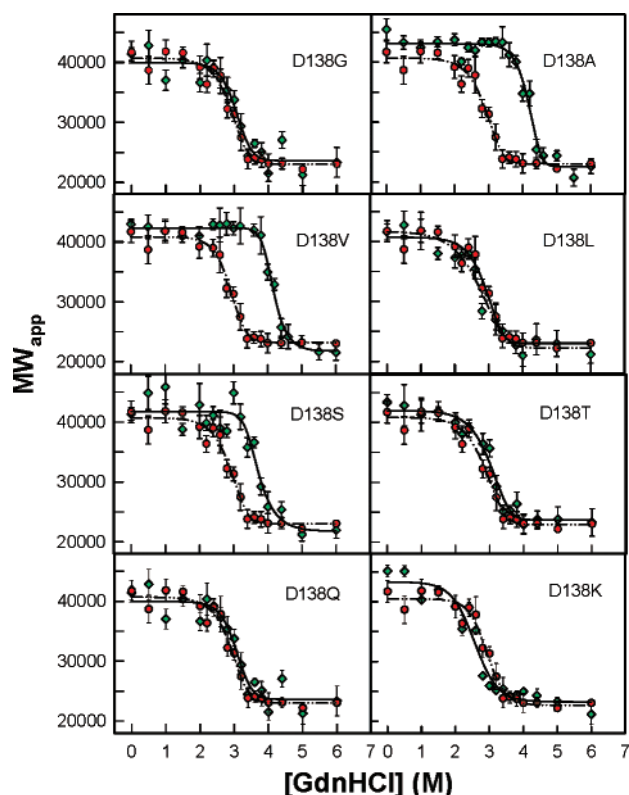

FIGURE 4: Apparent weight-average molecular weight of CRP as a function of GuHCl concentration: red circles and dashed lines for WT and green diamonds and solid lines for residue 138 mutants. The fitting curves are drawn to indicate the trend of the data.

Table 2: Subunit Association Data Monitored by Sedimentation Equilibrium

	$\Delta G_d°$ (kcal/mol)[a]	slope[b]	[GdnHCl]$_m$ (M)[c]
WT	11.7 ± 0.9	−2.1 ± 0.3	2.9
D138G	11.4 ± 0.8	−2.0 ± 0.3	3.1
D138A	18.6 ± 1.7	−3.2 ± 0.4	4.2
D138V	23.5 ± 1.7	−4.4 ± 0.4	4.2
D138L	11.8 ± 0.7	−2.3 ± 0.2	2.8
D138S	15.0 ± 1.4	−2.5 ± 0.4	3.7
D138T	13.5 ± 2.0	−2.7 ± 0.6	3.0
D138Q	13.0 ± 0.7	−2.8 ± 0.8	2.8
D138K	11.4 ± 0.8	−2.3 ± 0.3	2.6

[a] ΔG_d (dissociation energy change) = $-RT \ln K_d$. $\Delta G_d°$ is the extrapolated ΔG_d in the absence of denaturant. [b] Slope of ΔG_d vs concentration of GdnHCl in the transition region. [c] [GdnHCl]$_m$ is the concentration of GuHCl at which the MW$_{app}$ value indicates a 50% mixture of monomer and dimer.

been shown to play a significant role in allosteric regulation in CRP (*30−33*). The hinge region has also been suggested to constitute part of the pathway on the basis of structural information and mutagenesis analysis (*7, 24*). The hinge region connects the two functional domains. It is conceivable that the hinge region could play a role in signal transmission between the two functional domains. *In vivo* studies of single-amino acid substitutions in the hinge region revealed that residue 138 might be involved in hinge reorientation and interhelical adjustment (*20*). Furthermore, pairwise amino

acid substitutions in and around the hinge reveal the transfer of the signal from the hinge to the DNA binding domain via interaction between residue 138 and G141 (adjacent to the hinge and located at D-helix) (*21*). D138 is located in the groove that is formed by the two subunits, and it is partially exposed to solvent. It is reasonable to hypothesize that this location is affected by the side chain solvation ability. These multiple intricate interactions most likely constitute part of the complicated signal transmission pathway.

It is essential to elucidate the physical principles that govern this intricate network of allosteric communication. In this study, eight mutations of residue 138 were generated. These mutants include side chains of different physical properties such as hydrophobic, polar, and positively charged side chains. According to the CD spectroscopy of all these mutants, mutations of residue 138 do not change the net composition of the secondary and tertiary structure of CRP; however, the functional energetics of DNA binding, protein stability, and subunit assembly are significantly perturbed. Thus, subtle perturbations of structure are manifested as significant alterations in the functional and structural energetics of CRP.
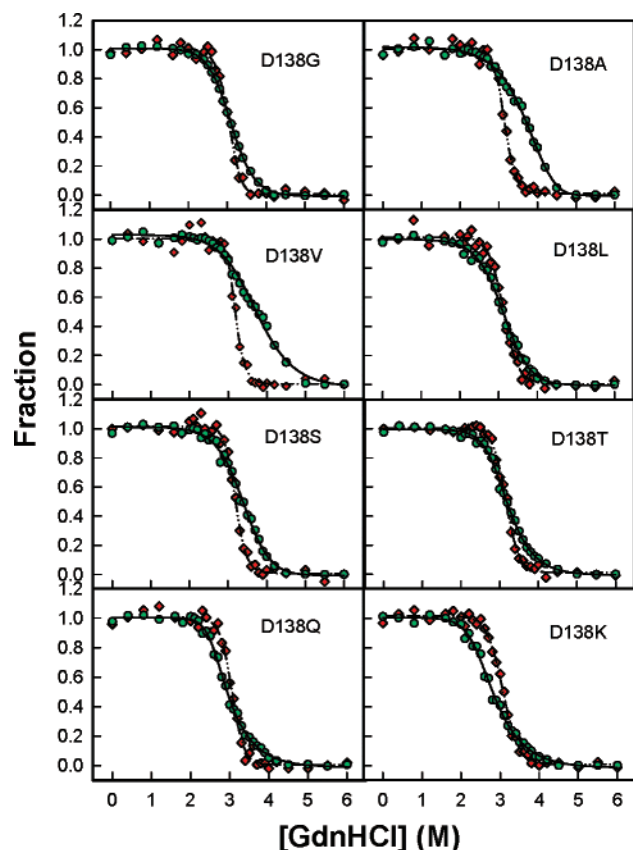
FIGURE 5: Unfolding curve monitored by fluorescence intensity (red diamonds) and circular dichroism (green circles). The solid line represents the trend of the data.

Residue 138 is not located in the DNA binding domain, yet structural perturbation due to mutations of this residue is transmitted to the F-helix, the DNA recognition helix, through long-range interactions, leading to measurable changes in DNA binding affinity (Table 1). The apparent DNA binding constant is related to the amino acid side chain. Replacing D138 with a positively charged side chain residue leads to DNA sequence binding affinities higher than that of WT, regardless of the specific sequence of the DNA. Substituting D138 with a polar side chain leads to a binding affinity close to that of WT. A replacement of D138 with a hydrophobic side chain yields a CRP which exhibits a binding affinity significantly lower than that of WT. These phenomena imply that DNA binding affinity is related to the side chain hydrophobicity of residue 138. An approximately linear correlation could be established between ΔG_{trans} and ΔG of CRP−DNA binding in the presence of 200 μM cAMP, as shown in Figure 6. There is a decrease in the free energy change of the DNA−CRP interaction with an increase in side chain hydrophobicity at position 138. There might be several reasons for the lack of a better observed linear correlation. (1) The chemical environment of each side chain depends on its neighbors and possibly on its covalent linkage to a multipeptide backbone. (2) The side chain is never fully exposed to the solvent because of the conformational flexibility of the polypeptide chain and the presence of the neighboring side chain (*34*). (3) The solvation energy of the peptide bond is uncertain. As a consequence, the solvation energy (ΔG_{trans}) can only be used as a semiquantitative estimation.

The hydrophobicity scale employed in this study is from the elegant work from the White laboratory (*35*). The free energy of transferring amino side chains from the organic phase to water, ΔG_{trans}, is generally derived from studies of the partitioning of model compounds that approximate single residues (*35, 36*). The free energy of transfer of acetyl amino acid amides (Ac-X-amide) from octanol into water is most commonly used (*35*), which is associated with the hydrophobicity of the protein side chain. White's lab assessed the octanol-to-water free energy transfer of the 20 natural amino acids (X) in the guest position of the host pentapeptide (AcWL-X-LL).

We established a linear correlation between the free energy difference in DNA−CRP binding in the presence of cAMP and cGMP, $\Delta\Delta G$, and the energetics of subunit association in a previous study (*24*), whose data indicate that an increase in subunit affinity is linked to an increase in the ability for CRP to distinguish cAMP from other cyclic nucleotides in affecting CRP in its interaction with specific DNA sequences. WT CRP occupies a position at the high end of the scale of $\Delta\Delta G$ and subunit affinity. That correlation implies that a quaternary constraint is required for CRP to distinguish among the various cyclic nucleotides. The current study found an approximately linear correlation between $\Delta\Delta G$ and the energetics of subunit assembly, with the exception of the D138L mutant, as shown in Figure 7. If the data for D138L are excluded, the mutant with higher energetics for subunit−subunit interaction has more difficulty binding to a specific DNA sequence, implying that the quaternary constraint leads to a constraint of the DNA binding domain. In this study, WT CRP occupies a position at the low end of the scale for subunit affinity but has a high $\Delta\Delta G$ value. From Figure 7, it is obvious that the degree of quaternary constraint embedded in WT CRP enables it to be most efficient in distinguishing among the cyclic nucleotides since it apparently is situated in the apex of this correlation.

It is interesting to correlate the protein stability, especially the stability of the cAMP binding domain, and DNA binding affinity. By comparing the DNA binding affinity and CRP stability data from fluorescence intensity, we obtained a linear correlation with an exception of the data for the D138L mutant, as shown in Figure 8. In CRP, the two tryptophan residues are located at positions 13 and 85, both in the β-roll of the cAMP binding domain. The protein stability information from the fluorescence study reflects probably mostly the stability of the cAMP binding domain. This linear correlation indicates that the more structural constraints there are in the cAMP binding domain, the more effective the DNA binding domain is in recognizing a specific DNA sequence. The specific mechanism and the reason for the exception of the D138L mutant are related to a specific perturbation of cAMP binding affinity to the "low-affinity" site.[2]

In summary, results from this *in vitro* study imply that residue 138 is part of the network for signal transmission between subunits and domains in CRP. The DNA binding affinity is linked to the energetics of subunit association. Furthermore, the more constrained the cAMP binding domain is, the lower the affinity for specific DNA becomes, an

---

[2] S. Yu and J. C. Lee, manuscript in preparation.

Table 3: Unfolding Data Monitored by Fluorescence and CD

	fluorescence			CD		
	$\Delta G_d^{\circ\,a}$	slope[b]	[GdnHCl]$_m$[c]	$\Delta G_d^{\circ\,a}$	slope	GdnHCl]$_m$
WT	9.2 ± 0.4	−2.9 ± 0.1	3.1	5.9 ± 0.2	−1.8 ± 0.1	3.1
D138G	12.3 ± 1.1	−4.0 ± 0.4	3.0	6.8 ± 0.2	−2.2 ± 0.1	3.1
D138A	14.9 ± 1.7	−4.7 ± 0.4	3.2	5.6 ± 0.2	−1.5 ± 0.1	3.7
D138V	18.1 ± 0.9	−5.6 ± 0.3	3.2	6.9 ± 0.3	−1.9 ± 0.1	3.7
D138L	10.1 ± 0.6	−3.2 ± 0.2	3.1	5.4 ± 0.2	−1.7 ± 0.1	3.1
D138S	12.0 ± 0.8	−3.8 ± 0.4	3.2	6.8 ± 0.3	−2.0 ± 0.1	3.4
D138T	11.4 ± 0.5	−3.6 ± 0.2	3.1	5.9 ± 0.2	−1.8 ± 0.1	3.2
D138Q	13.7 ± 1.4	−4.5 ± 0.4	3.1	5.8 ± 0.3	−1.9 ± 0.1	2.9
D138K	10.2 ± 0.6	−3.6 ± 0.2	3.1	4.6 ± 0.2	−1.6 ± 0.1	2.8

[a] ΔG_d (dissociation energy change) $= -RT \ln K_d$. ΔG_d° is the extrapolated ΔG_d in the absence of denaturant. [b] Slope of ΔG_d vs concentration of GdnHCl in the changing region. [c] [GdnHCl]$_m$ is the concentration of GuHCl at which 50% of the protein was unfolded.
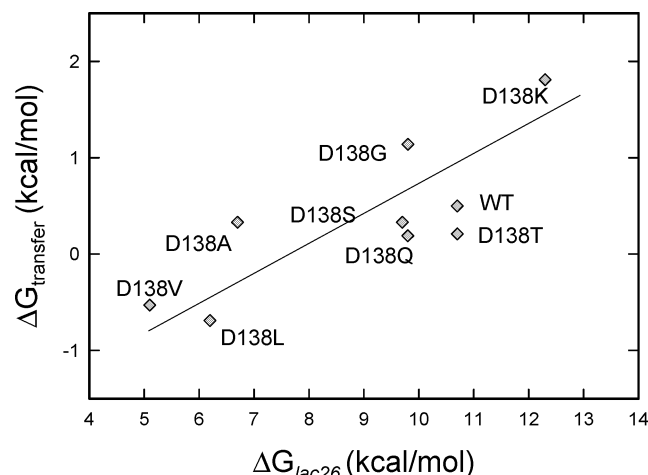

FIGURE 6: Relation between the free energy of transfer of the side chain from *n*-octanol to water and energetics of DNA binding to lac26 in the presence of 200 μM cAMP. The line is a linear least-squares regression with an *R* of 0.80.
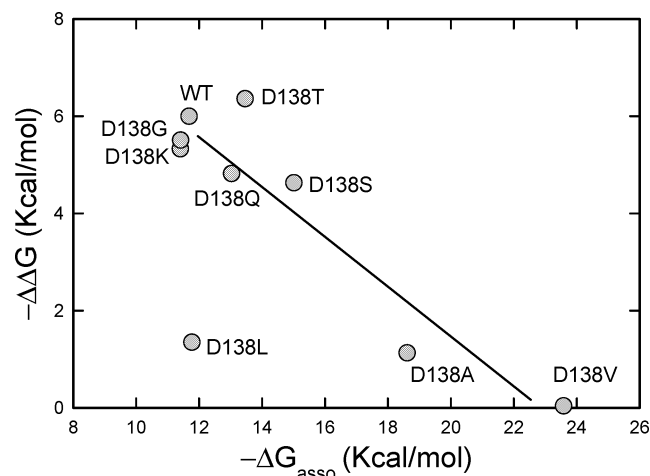

FIGURE 7: Relation between $\Delta\Delta G$, the difference in DNA binding in the presence of cAMP and cGMP, and the subunit association constant detected by the sedimentation equilibrium method.
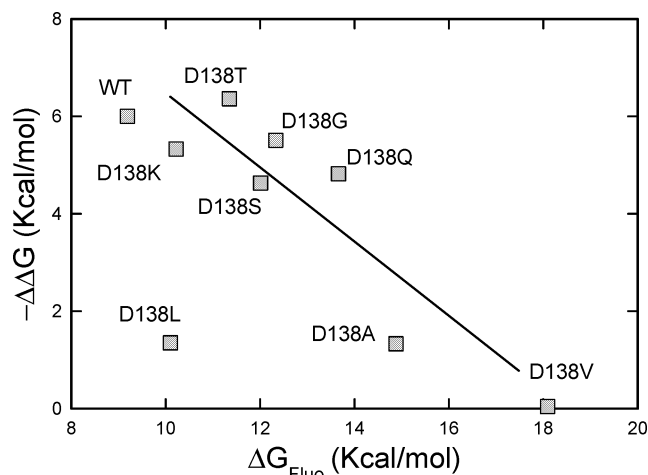

FIGURE 8: Relation between $\Delta\Delta G$ and the unfolding free energy change detected by the fluorescence intensity method.

through residue 138, and the nature of the interaction warrants further investigation. Results of this study clearly establish the importance of the linkages between structural stability and dynamics and the ability of CRP to manifest its intrinsic allosteric properties.

indication of the intimate structural and functional linkages among the domains and subunits. The correlation between the DNA binding and cAMP binding domains also indicates that the more constrained the cAMP binding domain is, probably the less dynamic the DNA binding domain becomes. The linear correlation between the hydrophobicity of the side chains of residue 138 and DNA binding affinity implies a general mechanism that governs signal transmission

REFERENCES

1. Adhya, S., and Garges, S. (1990) Positive control, *J. Biol. Chem. 265*, 10797−10800.
2. Busby, S., and Buc, H. (1987) Positive regulation of gene expression by cyclic AMP and its receptor protein in *Escherichia coli*, *Microbiol. Sci. 4*, 371−375.
3. De Crombrugghe, B., Busby, S., and Buc, H. (1984) Cyclic AMP Receptor Protein: Role in Transcription Activation, *Science 224*, 831−838.
4. Harman, J. G. (2001) Allosteric regulation of the cAMP receptor protein, *Biochim. Biophys. Acta 1547*, 1−17.
5. Cheng, X. D., and Lee, J. C. (1998) Interactive and Dominant Effects of Residues 128 and 141 on Cyclic Nucleotide and DNA Bindings in *E. coli* cAMP Receptor Protein, *J. Biol. Chem. 273*, 705−712.
6. Kumar, S. A., Murthy, N. S., and Krakow, J. S. (1980) Ligand-induced change in the radius of gyration of cAMP receptor protein from *Escherichia coli*, *FEBS Lett. 109*, 121−124.
7. Passner, J. M., Schultz, S. C., and Steitz, T. A. (2000) Modeling the cAMP-induced Allosteric Transition Using the Crystal Structure of CAP-cAMP at 2.1 Å Resolution, *J. Mol. Biol. 304*, 847−859.

8. Won, H.-S., Yamazaki, T., Lee, T.-W., Yoon, M.-K., Park, S.-H., Kyogoku, Y., and Lee, B. J. (2000) Structural Understanding of the Allosteric Conformational Change of Cyclic AMP Receptor Protein by Cyclic AMP Binding, *Biochemistry 39*, 13953−13962.

9. Lee, B. J., Aiba, H., and Kyogoku, Y. (1991) Nuclear magnetic resonance study on the structure and interaction of cyclic AMP receptor protein and its mutants: a deuterium-labeling and photo-CIDNP study, *Biochemistry 30*, 9047−9054.

10. Eilen, E., Pampeno, C., and Krakow, J. S. (1978) Production and properties of the α core derived from the cyclic adenosine monophosphate receptor protein of *Escherichia coli*, *Biochemistry 33*, 2469−2473.

11. Heyduk, T., and Lee, J. C. (1990) Application of fluorescence energy transfer and polarization to monitor *Escherichia coli* cAMP receptor protein and *lac* promoter interaction, *Proc. Natl. Acad. Sci. U.S.A. 87*, 1744−1748.

12. Cheng, X. D., Kovac, L., and Lee, J. C. (1995) Probing the Mechanism of CRP Activation by Site-Directed Mutagenesis: The Role of Serine 128 in the Allosteric Pathway of cAMP Receptor Protein Activation, *Biochemistry 34*, 10816−10826.

13. Baichoo, N., and Heyduk, T. (1997) Mapping Conformational Changes in a Protein: Application of a Protein Footprinting Technique to cAMP-Induced Conformational Changes in cAMP Receptor Protein, *Biochemistry 36*, 10830−10836.

14. Baichoo, N., and Heyduk, T. (1999) Mapping cyclic nucleotide-induced conformational changes in cyclic-AMP receptor protein by a protein footprinting technique using different chemical proteases, *Protein Sci. 8*, 518−528.

15. Wu, C.-W., and Wu, F. Y.-H. (1974) Conformational Transitions of Cyclic Adenosine Monophosphate Receptor Protein of *Escherichia coli*, *Biochemistry 13*, 2573−2578.

16. Passner, J. G., and Steiz, T. A. (1997) The structure of a CAP-DNA complex having two cAMP molecules bound to each monomer, *Proc. Natl. Acad. Sci. U.S.A. 94*, 2843−2847.

17. Weber, I. T., and Steitz, T. A. (1987) Structure of a Complex of Catabolite Gene Activator Protein and Cyclic AMP Refined at 2.5 Å Resolution, *J. Mol. Biol. 198*, 311−326.

18. Schultz, S. C., Shields, G. C., and Steitz, T. A. (1991) Crystal Structrue of a CAP-DNA Complex: The DNA Is Bent by 90°, *Science 253*, 1001−1007.

19. Heyduk, E., Heyduk, T., and Lee, J. C. (1992) Intersubunit Communications in *Escherichia coli* Cyclic AMP Receptor Protein: Studies of the Ligand Binding Domain, *Biochemistry 31*, 3682−3688.

20. Garges, S., and Adhya, S. (1988) Cyclic AMP-Induced Conformational Change of Cyclic AMP Receptor Protein (CRP): Intragenic Suppressors of Cyclic AMP-Independent CRP Mutations, *J. Bacteriol. 170*, 1417−1422.

21. Kim, J., Adhya, S., and Garges, S. (1992) Allosteric changes in the cAMP receptor protein of *Escherichia coli*: Hinge reorientation, *Proc. Natl. Acad. Sci. U.S.A. 89*, 9700−9704.

22. Ryu, S., Kim, J., Adhya, S., and Garges, S. (1993) Pivotal role of amino acid at position 138 in the allosteric hinge reorientation of cAMP receptor protein, *Proc. Natl. Acad. Sci. U.S.A. 90*, 75−79.

23. Cheng, X. D., and Lee, J. C. (1998) Differential Perturbation of Intersubunit and Interdomain Communications by Glycine 141 Mutation in *E. coli* CRP, *Biochemistry 37*, 51−60.

24. Chen, R., and Lee, J. C. (2003) Functional Roles of Loops 3 and 4 in the Cyclic Nucleotide Binding Domain of Cyclic AMP Receptor Protein from *Escherichia coli*, *J. Biol. Chem. 278*, 13235−13243.

25. Lin, S.-H., Kovac, L., Chin, A. J., Chin, C. C. Q., and Lee, J. C. (2002) Ability of *E. coli* Cyclic AMP Receptor Protein To Differentiate Cyclic Nucleotides: Effects of Single Site Mutations, *Biochemistry 41*, 2946−2955.

26. Lin, S.-H. and Lee, J. C. (2002) Communications between the High-Affinity Cyclic Nucleotide Binding Sites in *E. coli* Cyclic AMP Receptor Protein: Effect of Single Site Mutations, *Biochemistry 41*, 11857−11867.

27. Cheng, X. D., and Lee, J. C. (1994) Absolute requirement of cyclic nucleotide in the activation of the G141Q mutant cAMP receptor protein from *Escherichia coli*, *J. Biol. Chem. 269*, 30781−30784.

28. Cheng, X. D., Gonzalez, M. L., and Lee, J. C. (1993) Energetics of Intersubunit and Intrasubunit Interactions of *Escherichia coli* Adenosine Cyclic 3′,5′-Phosphate Receptor Protein, *Biochemistry 32*, 8130−8139.

29. Cohn, E. J., and Edsall, J. T. (1943) in *Protein, Amino Acids and Peptides*, p 372, Van Nostrand-Reinhold, Princeton, NJ.

30. Garges, S., and Adhya, S. (1985) Sites of Allosteric Shift in the Structure of the Cyclic AMP Receptor Protein, *Cell 41*, 745−751.

31. Bell, A., Gaston, K., Williams, R., Chapman, K., Kolb, A., Buc, H., Minchin, S., Williams, J., and Busby, S. (1990) Mutations that alter the ability of the *Escherichia coli* cyclic AMP receptor protein to activate transcription, *Nucleic Acids Res. 18*, 7243−7250.

32. Tagami, H., and Aiba, H. (1998) Role of CRP in transcription activation at *Escherichia coli* lac promoter: CRP is dispensable after the formation of open complex, *Nucleic Acids Res. 25*, 599−605.

33. Harman, J. G., Peterkofsky, A., and McKenney, K. (1988) Arginine Substituted for Leucine at Position 195 Produces a Cyclic AMP-independent Form of the *Escherichia coli* Cyclic AMP Receptor Protein, *J. Biol. Chem. 263*, 8072−8077.

34. Creamer, T. P., Srinivasan, R., and Rose, G. D. (1995) Modeling unfolded states of peptides and proteins, *Biochemistry 34*, 16245−16250.

35. Wimley, W. C., Creamer, T. P., and White, S. H. (1996) Solvation Energies of Amino Acid Side Chains and Backbone in a Family of Host−Guest Pentapeptides, *Biochemistry 35*, 5109−5124.

36. Radzicka, A., and Wolfenden, R. (1988) Comparing the polarities of the amino acids: side-chain distribution coefficients between the vapor phase, cyclohexane, 1-octanol, and neutral aqueous solution, *Biochemistry 27*, 1664−1670.